# Chaotic Behavior of Fluidized Beds Based on Pressure and Voidage Fluctuations

**D. Bai, H. T. Bi, and J. R. Grace**
Dept. of Chemical Engineering, University of British Columbia, Vancouver, BC, Canada V6T 1Z4

Absolute and differential fluctuations and local voidage fluctuations are commonly used in characterizing gas-fluidized beds. Pressure fluctuations can result from several different causes including bubble formation and eruption, self-excited oscillations of fluidized particles, pressure oscillations in the plenum chamber due to piston-like motion of the bed, bubble coalescence, and bubble splitting (Bi et al., 1995). Pressure waves from these sources can be propagated through the emulsion phase, although the amplitudes of the signals are attenuated during their propagation (Bi et al., 1995). Therefore, an absolute pressure probe records phenomena on a macroscopic scale from other locations in addition to local variations. Differential pressure measurements can, to a limited extent, filter out pressure waves originating outside the interval between the two ports connected to the differential pressure transducer, that is, measurements are on a meso-scale. Voidage probes reflect local (that is, microscale) voidage variations caused by bubble passage and the particle movement of the emulsion phase. The amplitude of local voidage fluctuations is independent of bubble size, unlike pressure fluctuations whose amplitude increases with bubble size. Previous studies (Bi et al., 1995; Bi and Grace, 1995) have shown that statistical characteristics (such as standard deviation, skewness, dominant frequency, probability distribution) calculated from these three types of signals differ significantly from one another.

In recent years, the application of deterministic chaos theory to fluidized beds has been pioneered by several research groups (such as Daw and Halow, 1991; van den Bleek and Schouten, 1993; Skrzycke et al., 1993; Halow and Daw, 1994; van der Stappen et al., 1995). Analysis of pressure fluctuation signals (such as the phase-space portrait, Lyapunov exponent, correlation dimension, and Kolmogorov entropy) has provided evidence that gas-solids fluidized beds are deterministic chaotic systems. The correlation dimension of the time series has been calculated based on time series from absolute (van der Stappen et al., 1993) and differential (Daw and Halow, 1991) pressure fluctuation measurements. In view of the different information contained in time traces of absolute and differential pressure and local voidage, this article examines the chaotic characteristics of signals from these three measurement methods based on analysis of signals recorded simultaneously in gas-solids fluidized beds.

## Experiments

The experiments were carried out in a 102-mm-dia. column described previously (Bi and Grace, 1995). Both FCC particles of $\bar{d}_p = 60\ \mu$m, $\rho_p = 1{,}580$ kg/m$^3$ and sand particles of $\bar{d}_p = 214\ \mu$m, $\rho_p = 2{,}640$ kg/m$^3$ were used in the tests with the static bed height maintained at 0.6 m for all tests. ($\bar{d}_p$ is the mean particle diameter and $\rho_p$ is the particle density.) Three gas velocities were used, corresponding to different flow regimes. Pressure fluctuations were measured from ports on the wall of the column using Omega PX162 pressure transducers. A low-pass filter eliminates signals with frequencies above 20 Hz. Absolute pressure fluctuations and local voidages were measured 0.28 m above the distributor, while differential pressure fluctuations were measured across an interval from 0.20 to 0.41 m above the distributor. The optical probe (see Zhou et al., 1994 for details) was located with its 1.5 mm tip on the axis of the column. All signals were sampled by a digital data logging system (12 bit DAS 8 A/D board, Labtech Notebook data acquisition software) at a frequency of 100 Hz for intervals of 40 s. A low-pass filter set at 20 Hz was used in the pressure fluctuation measurements, and each data set was numerically smoothed to eliminate small amplitude high frequency noise components before data analysis.

## Results and Discussion

### *Power spectra*

The power spectrum of a chaotic time series is quite different from those of periodic and quasi-periodic time series. The former has a continuous, broad band noise-like spectrum. $S$ is the power spectrum intensity. Beyond a certain frequency ($f$, Hz) range the power spectrum intensity decays with frequency, obeying a power law

$$S(f) \propto f^{-K} \tag{1}$$

Correspondence concerning this article should be addressed to J. R. Grace.

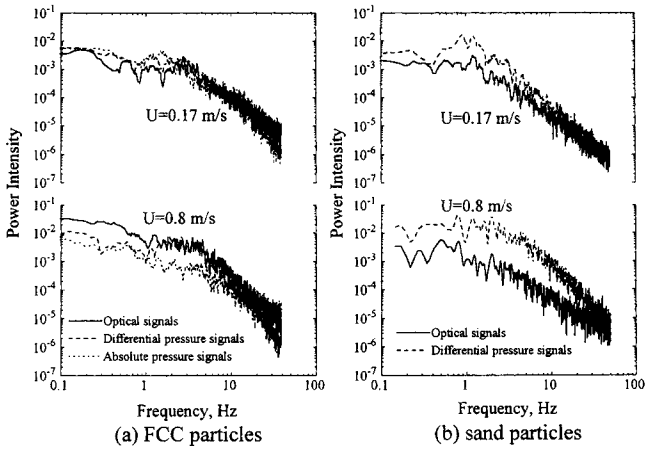


**Figure 1. Power spectrum distribution of absolute and differential pressure fluctuations and of local voidage fluctuations for (a) FCC particles, and (b) sand particles.**

(Moon, 1992). A large value of the exponent $K$ indicates that the intensity drops quickly with little high frequency content and lower fractal dimension (Xia et al., 1992; Drahos et al., 1992; Bai et al., 1996a). Power spectra were calculated for the three types of fluctuation signals using normalized measurements, that is, the mean was subtracted followed by division by the standard deviation. Figure 1 shows that for both types of particle the power spectral distributions of the three types of fluctuation signals are similar at a low superficial gas velocity $u$ of 0.17 m/s, while there are greater differences for $U = 0.8$ m/s.

Figure 2 shows the effect of superficial gas velocity on $K$ from the three different types of signals. Values of $K$ from absolute and differential pressure fluctuations are seen to be quite close to each other and, except at very low $U$, to be higher than $K$ derived from local voidage fluctuations (that is, optical probe signals), implying that the latter contain less high frequency content than absolute and differential pressure fluctuations.

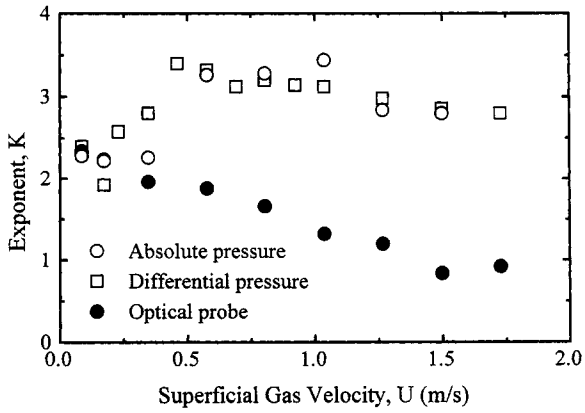


**Figure 2. Effects of superficial gas velocity and measurement method on decay constant $K$ for FCC particles.**

### *Lyapunov exponent*

Chaotic systems are sensitive to initial conditions. Small initial uncertainties or disturbances cause the system dynamics to be totally unpredictable beyond a certain time. The Lyapunov exponents measure the rates at which system processes create or destroy information. Any system with at least one positive Lyapunov exponent is defined as chaotic (Moon, 1992; Mullin, 1993).

Of several methods available in the literature for estimating the largest Lyapunov exponent (Sano and Sawada, 1985; Sato et al., 1987; Zeng et al., 1991), the method of Wolf et al. (1985) was adopted in this work. Details are provided by Wolf et al. (1985), Mullin (1993), and, for fluidization, by Hay et al. (1995). As stressed by Wolf et al. (1985), to reduce the influence of noise, points with a distance greater than some predetermined noise threshold are selected on a trajectory of the phase portrait embedded in a $d$-dimensional phase space. Since the noise scale is unknown in advance, the threshold length was adjusted in this study until a relatively constant estimate of the largest Lyapunov exponent was achieved. The calculations demonstrated that the estimates of the Lyapunov exponent became almost constant when evolution time was increased. The largest Lyapunov exponents were then obtained by averaging estimates at several higher evolution times, and the error bands were taken from the maximum and minimum values at the same time. Figure 3 shows the estimated largest Lyapunov exponents for the two types of particle based on the three different measured signals at three superficial gas velocities. The positive Lyapunov exponents help confirm that the systems are chaotic. The minima in the Lyapunov exponent curves may correspond to transition from bubbling to turbulent fluidization. A similar trend was reported by Daw and Halow (1991) for the Kolmogorov entropy, a measure equivalent to the Lyapunov exponent. We have also found similar trends with respect to Kolmogorov entropies calculated from the same raw data (Bai et al., 1996b).

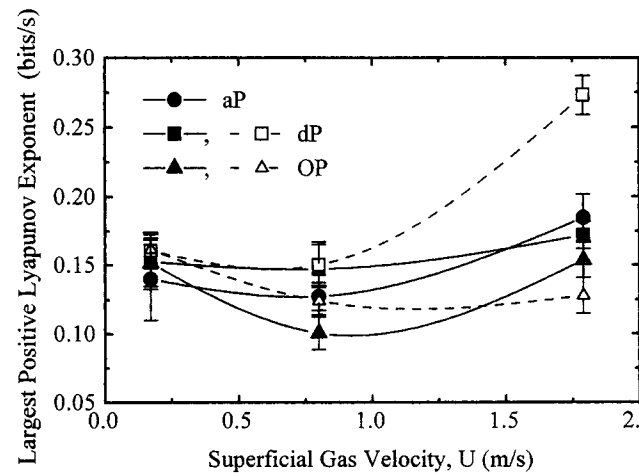


**Figure 3. Effect of gas velocity and measurement method on the Lyapunov exponent for FCC (black symbols) and sand particles (open symbols).**

aP denotes absolute pressure; dP stands for differential pressure; OP indicates optical probe measurements.

Note that the Lyapunov exponents for the same gas velocity differ for the three types of signals. The fluctuating pressure signals seem to be most sensitive to initial conditions, judging from their highest values of the Lyapunov exponent. The exponent is generally lowest for the optical probe, which detects local voidage signals that appear to be less complex than the more broadly based pressure fluctuations signals.

### *Correlation dimension*

Several fractal dimensions have been proposed in the literature including the capacity dimension, information dimension and correlation dimension (Moon, 1992). For time-series analysis, the correlation dimension is commonly used. For a time series $x_i$ ($i=1$ to $N$), we can reconstruct a $d$-dimensional space with $M$ points $\{X_i\}$ in the phase space. $M$ is the length of vector $X_i$ and $N$ is the number of points. The distances between pairs of points, $\| X_i - X_j \|$ can then be calculated ($i$ and $j$ are integers). A correlation integral is next defined (Grassberger and Procaccia, 1983)

$$C(r) = \lim_{M \to \infty} \frac{1}{M^2} \{\text{number of pairs of points } (i,j) \text{ with distance } \| X_i - X_j \| < r\} \quad (2)$$

where $X_i$ is the $d$-dimensional reconstructive vector, defined as

$$X_i = \{x_i, x_{i+\tau}, \ldots, x_{i+(d-1)\tau}\} \quad (i = 1,2,\ldots,M) \quad (3)$$

It can be shown that $C(r)$ is proportional to $r^{Dc}$ when $r$, the radius of the hypersphere, is small compared with the size of the attractor. The correlation dimension is then defined as

$$D_c = \lim_{r \to 0} \frac{\ln C(r)}{\ln r} \quad (4)$$

The usual practice is to select random pairs of ($X_i$, $X_j$). A plot of $\log(C(r))$ vs. $\log(r)$ is then produced for a given embedding dimension, and the correlation dimension is calculated from the slope of the linear part. The embedding dimension of the attractor is then increased and another correlation dimension is calculated. The slope or correlation dimension becomes independent of embedding dimension when the latter is sufficiently large.

To calculate the correlation integral from Eq. 2 and to evaluate the correlation dimension using Eq. 4, several aspects need to be considered:

*(a) Number of Data Points.* The number of data points is an important parameter which has been subject to debate (van den Bleek and Schouten, 1993; Schouten et al., 1994). A sufficient number of points is needed to ensure accuracy. A number of authors have shown that 4,000 to 10,000 points are generally sufficient for multiphase flow systems. In a bubble column, Drahos et al. (1992) found 3,000 points to be sufficient, while Hay et al. (1995) found 5,000 points to be sufficient for bubbling fluidized beds. In our cases, reasonable estimates of the correlation dimension could be reached using 4,000 data points as long as the vector size was sufficiently large (i.e., $M = 1{,}000$). This number also satisfies the criterion proposed by Ruelle (1990) that $10^{Dc/2}$ points are required. Greater precision in the $D_c$ values could have been obtained, however, by taking a large number of points.

*(b) Delay Time.* Various rules are given in the literature regarding the choice of the delay time. Grassberger and Procaccia (1983) and Tam and Devine (1991) suggested that it be based on the first zero-crossing, the first minimum of the autocorrelation function, or the first minimum of the mutual information function. On the other hand, van den Bleek and Schouten (1993) chose the time delay as simply the time interval between successive points in their time series. In our case for $d = 15$ with $M = 1{,}000$ (randomly selected) and calculations repeated twenty times, $\log(C(r))/\log(r)$ converges to a constant value when the time delay is greater than about 0.11 s, similar to the first zero-crossing time of the autocorrelation function or the time of the first minimum of the autocorrelation function, whichever occurs first. The delay time has therefore been based on this criterion.

*(c) Embedding Dimension.* The dimension of the embedding state space should be large enough to encompass the complete reconstructed attractor. Takens (1981) showed that embedding with $d \geq 2D_c + 1$ is sufficient to ensure faithful complete evolution of the attractor in reconstructed state space. In this study, a constant slope is observed at $d \approx 12$. A higher value $d = 15$ has been utilized in this work. In most cases, this also satisfies Takens' criterion.

*(d) Effect of Noise.* Time signals from natural phenomena are subject to noise which can significantly increase the correlation dimension in nonlinear time-sequence analysis (Lacy et al., 1991). In this study, a low-pass filter set at 20 Hz has been used in data sampling. In addition, numerical smoothing was applied to further eliminate low amplitude and high frequency noise.

Typical logarithmic plots of $C(r)$ vs. $r$ for FCC particles using the standard Grassberger-Procaccia (1983) method appear in Figure 4a. To reduce the autocorrelation effect that may exist for limited time-series data, Theiler (1986) modified the standard Grassberger and Procaccia algorithm by introducing a cutoff parameter $W$, thereby improving the convergence of the standard correlation algorithm toward its $N \to \infty$ limit. This modification is incorporated in Figure 4b with $W = 12$. Whether or not the Theiler modification is included, there exist two distinct linear sections of nonzero slope separated by a transition region, except for the optical signals at $U = 1.73$ m/s where the two slopes at low $r$ appear to converge. Except in the last case, two correlation dimensions can be derived from each curve with correlation coefficients higher than 0.98. The higher dimension at a small scale probably corresponds to particle motion, which generates high frequency, small-scale voidage oscillations in the dense phase. The lower dimension at a large scale probably results from the motion of voids, which generate low frequency, large-scale fluctuations. For FCC particles at $U = 1.73$ m/s, the local flow structure in the bed center is dominated by dispersed particles and only one correlation dimension is identified from the optical probe.

The correlation dimensions are given in Table 1 for the three measurement methods and different operating conditions. The error bands were given by the numerical regres-

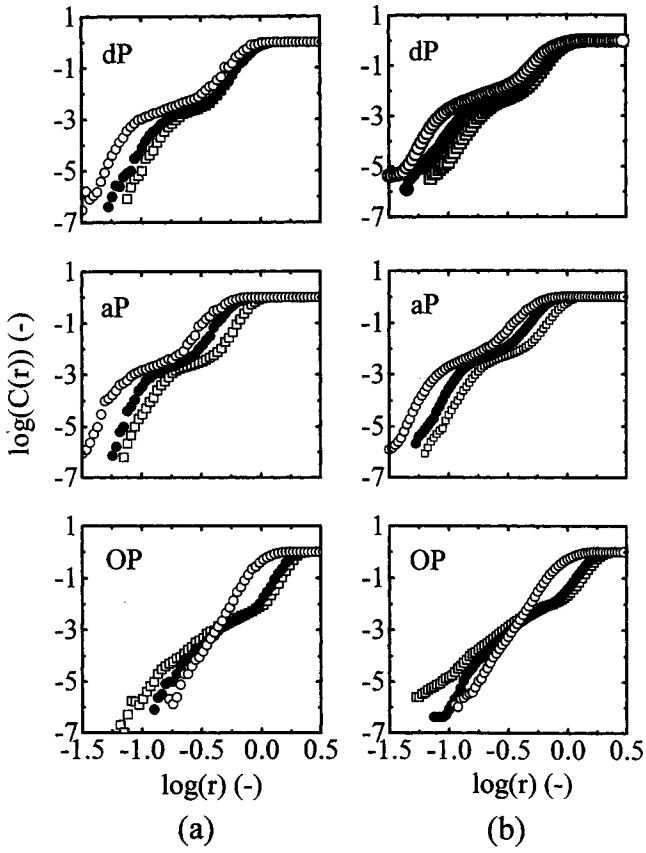


**Figure 4. Logarithmic plots of correlation integral as a function of radius for FCC particles: (a) standard Grassberger-Procaccia method (1983); (b) modified Grassberger-Procaccia method (Thieler, 1986) ($W = 12$).**

Delay time is derived from the first zero-crossing time of the autocorrelation function; $d = 15$. Open squares: $U = 0.17$ m/s; solid circles: $U = 0.8$ m/s; open circles: $U = 1.73$ m/s. *aP* denotes absolute pressure fluctuations; dP denotes differential pressure fluctuations; OP denotes local voidage fluctuations.

sion of the linear parts of the correlation integral curves, and correspond to 95% confidence intervals. The values of $D_{c1}$ for both absolute and differential pressure fluctuations are seen to be quite close to each other and to be higher than those corresponding to local voidage fluctuations measured by the optical probe. With increasing superficial gas velocity, $D_{c1}$ appears to reach a minimum at the transition from the bubbling to the turbulent fluidization regime. $D_{c2}$ generally decreases as the superficial gas velocity is increased as the bed passes from bubbling through slugging to the turbulent and fast fluidization regimes, that is, the bubble motion becomes less predominant. Both $D_{c1}$ and $D_{c2}$ are higher for FCC particles than for sand, suggesting greater complexity of fluidization for group A particles than for group B particles.

## Discussion

To confirm the multiple slopes in the correlation integral plots, a method similar to that of Ben-Mizrachi et al. (1984), who added low-amplitude random noise to deterministic chaos (using the Lorenz attractor), was generated and analyzed with our computer program. The superimposed nature of the signal was revealed, with the part related to the noise showing an increasing slope with increasing embedding dimension, while the part arising from the Lorenz attractor corresponded to the correct correlation dimension of $D_c = 2.16$. In our case we conjecture that the two slopes arise from the separate phases of low-velocity fluidized beds. Two-phase gas-liquid flows have also been reported to be multidimensional (Franca et al., 1991; Izrar and Lusseyran, 1993). Franca et al. (1991) identified two correlation dimensions in the annular flow regime for horizontal transport. The authors speculated that large-scale signals ($D_{c2} \approx 1$) came from surface waves while small-scale signals ($D_{c1} \approx 6$) originated from rolling waves. Izrar and Lusseyran (1993) identified two correlation dimensions in a countercurrent vertical transport line, with $D_{c1} \approx 7$ for small-scale signals and $D_{c2} \approx 3$ for large-scale signals. The small-scale signals were attributed to waves of small amplitude from turbulent film flow, while the large-scale signals were ascribed to liquid surface waves.

Bubbling and slugging gas-solids fluidized beds consist of two distinct phases: a bubble/void phase and an emulsion phase. It has been shown (van den Bleek and Schouten, 1993; Daw and Halow, 1991) that both particle motion and bubble motion can produce chaotic behavior. The optical fiber probe registers fluctuations from both the voids and the emulsion phase, with large-scale low frequency signals from bubble motion superimposed on small-scale, high frequency signals from the particle/emulsion motion. Absolute and differential pressure fluctuations, on the other hand, are dominated by signals from bubbles inside (and, in the case of absolute pressure measurements, outside) the measurement interval. $D_{c1}$ from the optical fiber probe is less than from the differential pressure fluctuation measurements, suggesting that the high frequency small-scale pressure waves are more complex than

**Table 1. Estimated Properties and Dimensions for FCC and Sand Particles in Different Fluidization Regimes**

| $U$ (m/s) | Probe | Voidage* | $K$ | $D_{c1}$ | $D_{c2}$ | Flow Regime** |
|---|---|---|---|---|---|---|
| | | | FCC Particles | | | |
| 0.17 | aP | NA | 3.5 | 7.76±0.43 | 6.55±0.19 | Bubbling |
| | dP | 0.49 | 1.9 | 7.25±0.31 | 6.42±0.17 | |
| | OP | 0.60 | 2.2 | 5.86±0.24 | 6.18±0.20 | |
| 0.80 | aP | NA | 2.9 | 7.32±0.34 | 6.42±0.16 | Turbulent |
| | dP | 0.55 | 3.2 | 6.17±0.37 | 5.16±0.22 | |
| | OP | 0.65 | 1.6 | 5.61±0.30 | 6.23±0.15 | |
| 1.73 | aP | NA | 2.3 | 7.51±0.55 | 5.78±0.35 | Fast |
| | dP | 0.74 | 2.8 | 7.42±0.39 | 5.03±0.28 | |
| | OP | 0.84 | 0.9 | 7.74±0.12 | — | |
| | | | Sand Particles | | | |
| 0.17 | dP | 0.49 | 2.6 | 6.81±0.12 | 5.67±0.08 | Bubbling |
| | OP | 0.67 | 2.1 | 5.60±0.09 | 5.16±0.15 | |
| 0.80 | dP | 0.54 | 2.7 | 4.94±0.10 | 4.75±0.05 | Slugging |
| | OP | 0.75 | 2.0 | 4.82±0.07 | 5.20±0.09 | |
| 1.79 | dP | 0.63 | 2.2 | 5.34±0.18 | 4.13±0.03 | Turbulent |
| | OP | 0.79 | 1.7 | 6.04±0.15 | 5.64±0.12 | |

*Voidage is expected to be larger for the OP signals since these are local values along the axis of the column while dP signals reflect the entire cross section.
**Based on correlations of Bi and Grace (1995) and Bi et al. (1995).
aP denotes absolute pressure; dP denotes differential pressure; OP denotes optical probe; NA is not applicable.

the local voidage oscillations. Beyond the turbulent regime, much of the two-phase character is lost, and this may explain the single correlation dimension for FCC particles at the highest $U$.

## Conclusions

Differences between absolute and differential pressure fluctuations and local voidage fluctuations lead to significant differences in power spectrum distribution diagrams, autocorrelation function diagrams, largest Lyapunov exponents, and correlation dimensions. Local voidage traces include both small-scale, high-frequency signals corresponding to local dense phase particle motion and low frequency, large-scale fluctuations due to the passage of voids and large-scale aggregates. Pressure fluctuation measurements reflect bubble motion and local disturbances induced by void interactions and propagating pressure waves. Two correlation dimensions are found in bubbling, slugging, and turbulent fluidized beds. The higher one, corresponding to small-scale fluctuations, probably represents particle motion and local turbulence, while the lower one, corresponding to large-scale fluctuations, reflects bubble motion or other large-scale phenomena.

## Acknowledgment

The authors are grateful to the Natural Sciences and Engineering Research Council of Canada for supporting this work.

## Literature Cited

Bai, D., Y. Masuda, N. Nakagawa, and K. Kato, "Hydrodynamics of a Binary Solids Fluidized Bed," *J. Chem. Eng. Japan*, **29,** 211 (1996a).

Bai, D., H. T. Bi, and J. R. Grace, "Dependence of Chaotic Behaviour of Fluidized Beds on Experimental Measurement Methods," *Proc. Int. Conf. on Fractal Concepts and Application of Chaos in Chem. Eng. Problems,* Rome, Italy (1996b).

Ben-Mizrachi, A., I. Procaccia, and P. Grassberger, "Characterization of Experimental (Noisy) Strange Attractors," *Phys. Rev. A.*, **29,** 975 (1984).

Bi, H. T., J. R. Grace, and J. X. Zhu, "Propagation of Pressure Waves and Forced Oscillation of Fluidized Beds and their Effects on Measurements of Local Hydrodynamics," *Powder Technol.*, **82,** 239 (1995).

Bi, H. T., and J. R. Grace, "Effects of Measurement Method on Velocities Used to Demarcate the Onset of Turbulent Fluidization," *Chem. Eng. J.*, **57,** 261 (1995).

Daw, C. S., and J. S. Halow, "Characterization of Voidage and Pressure Signals from Fluidized Beds Using Deterministic Chaos Theory," *Proc. Fluidized Bed Combustion*, **2,** 777 (1991).

Drahos, J., F. Bradka, and M. Puncachar, "Fractal Behaviour of Pressure Fluctuations in a Bubble Column," *Chem. Eng. Sci.*, **47,** 4069 (1992).

Franca, F., M. Acikgoz, R. T. Lahey, Jr., and A. Clausse, "The Use of Fractal Techniques for Flow Regime Identification," *Int. J. Multiphase Flow*, **17,** 545 (1991).

Grassberger, P., and L. Procaccia, "Characterization of Strange Attractors," *Phys. Rev. Lett.*, **50,** 346 (1983).

Halow, J. S., and C. S. Daw, "Characterizing Fluidized-Bed Behaviour by Decomposition of Chaotic Phase-Space Trajectories," *AIChE Symp. Ser.*, **90** (301), 69 (1994).

Hay, J. M., B. H. Nelson, C. L. Briens, and M. A. Bergougnou, "The Calculation of the Characteristics of a Chaotic Attractor in a Gas-Solid Fluidized Bed," *Chem. Eng. Sci.*, **50,** 373 (1995).

Izrar, B., and F. Lusseyran, "Chaotic Behaviour of an Annular Film of Liquid Unstabilized by an Interfacial Shear Stress," *Instabilities in Multiphase Flows*, G. Gouesbet, ed., Plenum Press, New York, pp. 1–15 (1993).

Lacy, C. E., M. Sheituch, and A. E. Dukler, "Methods of Deterministic Chaos Applied to the Flow of Thin Wavy Films," *AIChE J.*, **37,** 481 (1991).

Moon, F. C., *Chaotic and Fractal Dynamics*, Wiley, New York (1992).

Mullin, T., *The Nature of Chaos*, Clarendon Press, Oxford (1993).

Ruelle, D., "Deterministic Chaos: The Science and the Fiction," *Proc. Roy. Soc. Lond. A*, **427,** 241 (1990).

Sano, M., and Y. Sawada, "Measurement of the Lyapunov Spectrum from Chaotic Time Series," *Phys. Rev. Lett.*, **55,** 1082 (1985).

Sato, S., M. Sano, and Y. Sawada, "Practical Methods of Measuring the Generalized Dimension and the Largest Lyapunov Exponent in High Dimensional Chaotic Systems," *Prog. Theor. Phys.*, **77,** 1 (1987).

Schouten, J. C., F. Takens, and C. M. van den Bleek, "Maximum-Likelihood Estimation of the Entropy of an Attractor," *Phys. Rev. E*, **49,** 126 (1994).

Skrzycke, D. P., K. Nguyen, and C. S. Daw, "Characterization of the Fluidization Behaviour of Different Solid Types Based on Chaotic Time Series Analysis of Pressure Signals," *Proc. Fluidized Bed Combustion*, **1,** 155 (1993).

Takens, F., *Lecture Notes in Mathematics*, Vol. 898, Springer, New York, p. 366 (1981).

Tam, S. W., and M. K. Devine, "Is There a Strange Attractor in a Fluidized Bed?" *Measures of Complexity and Chaos*, N. B. Abraham, A. M. Albano, A. Passamante, and P. E. Rapps, eds., Plenum Press, New York, p. 193 (1991).

Theiler, J., "Spurious Dimension from Correlation Algorithm Applied to Limited Time-Series Data," *Phys. Rev. A.*, **34** 2427 (1986).

van den Bleek, C. M., and J. C. Schouten, "Deterministic Chaos: a New Tool in Fluidized Bed Design and Operation," *Chem. Eng. J.*, **53,** 75 (1993).

van der Stappen, M. L. M., J. C. Schouten, and C. M. van den Bleek, "Deterministic Chaos Analysis of the Dynamical Behaviour of Slugging and Bubbling Fluidized Beds," *Proc. Fluidized Bed Combustion*, **1,** 129 (1993).

van der Stappen, M. L. M., J. C. Schouten, and C. M. van den Bleek, "Chaotic Hydrodynamics and Scale-Up of Gas-Solids Fluidized Beds - Using the Kolmogorov Entropy for Quantification," *Preprints for Fluidization VIII*, Tours, France (May 14–19, 1995).

Wolf, A., J. B. Swift, H. L. Swinney, and J. A. Vastano, "Determining Lyapunov Exponents from a Time Series," *Physica D*, **16,** 285 (1985).

Xia, Y., C. Zheng, and H. Li, "Characterizing Fast Fluidization by Optic Output Signals," *Powder Technol.*, **72,** 1 (1992).

Zeng, X., R. Eykholt, and R. A. Pielke, "Estimating the Lyapunov Exponent from Short Time Series of Low Precision," *Phys. Rev. Lett.*, **66,** 3229 (1991).

Zhou, J., J. R. Grace, S. Qin, C. H. M. Brereton, C. J. Lim, and J.-X. Zhu, "Voidage Profiles in a Circulating Fluidized Bed of Square Cross-Section," *Chem. Eng. Sci.*, **48,** 3217 (1994).

*Manuscript received Feb. 12, 1996, and revision received Dec. 5, 1996.*